AMERICAN SOCIETY FOR MICROBIOLOGY | Antimicrobial Agents and Chemotherapy®

ANTIVIRAL AGENTS

Population Pharmacokinetic Modeling To Estimate the Contributions of Genetic and Nongenetic Factors to Efavirenz Disposition

Jason D. Robarge,[a] Ingrid F. Metzger,[a] Jessica Lu,[a] Nancy Thong,[a] Todd C. Skaar,[a] Zeruesenay Desta,[a] Robert R. Bies[a,b]

Indiana University School of Medicine, Division of Clinical Pharmacology, Indianapolis, Indiana, USA[a]; State University of New York at Buffalo, School of Pharmacy and Pharmaceutical Sciences, Buffalo, New York, USA[b]

ABSTRACT Efavirenz pharmacokinetics is characterized by large between-subject variability, which determines both therapeutic response and adverse effects. Some of the variability in efavirenz pharmacokinetics has been attributed to genetic variability in cytochrome P450 genes that alter efavirenz metabolism, such as *CYP2B6* and *CYP2A6*. While the effects of additional patient factors have been studied, such as sex, weight, and body mass index, the extent to which they contribute to variability in efavirenz exposure is inconsistently reported. The aim of this analysis was to develop a pharmacometric model to quantify the contribution of genetic and nongenetic factors to efavirenz pharmacokinetics. A population-based pharmacokinetic model was developed using 1,132 plasma efavirenz concentrations obtained from 73 HIV-seronegative volunteers administered a single oral dose of 600 mg efavirenz. A two-compartment structural model with absorption occurring by zero- and first-order processes described the data. Allometric scaling adequately described the relationship between fat-free mass and apparent oral clearance, as well as fat mass and apparent peripheral volume of distribution. Inclusion of fat-free mass and fat mass in the model mechanistically accounted for correlation between these disposition parameters and sex, weight, and body mass index. Apparent oral clearance of efavirenz was reduced by 25% and 51% in subjects predicted to have intermediate and slow CYP2B6 metabolizer status, respectively. The final pharmacokinetic model accounting for fat-free mass, fat mass, and CYP2B6 metabolizer status was consistent with known mechanisms of efavirenz disposition, efavirenz physiochemical properties, and pharmacokinetic theory. (This study has been registered at ClinicalTrials.gov under identifier NCT00668395.)

KEYWORDS body composition, cytochrome P450 2B6 (CYP2B6), efavirenz, population pharmacokinetics

Received 18 August 2016 **Returned for modification** 17 September 2016 **Accepted** 22 October 2016

Accepted manuscript posted online 31 October 2016

Citation Robarge JD, Metzger IF, Lu J, Thong N, Skaar TC, Desta Z, Bies RR. 2017. Population pharmacokinetic modeling to estimate the contributions of genetic and nongenetic factors to efavirenz disposition. Antimicrob Agents Chemother 61:e01813-16. https://doi.org/10.1128/AAC.01813-16.

Address correspondence to Zeruesenay Desta, zdesta@iu.edu.

Efavirenz is a nonnucleoside reverse transcriptase inhibitor that is used in combination with nucleoside/nucleotide reverse transcriptase inhibitors to treat HIV-infected individuals older than 3 years who are naive to antiretroviral drugs. Due to its proven efficacy and low cost relative to newer antiretrovirals, efavirenz-based therapy remains the preferred first-line regimen in many low-income nations and is consequently one of the most commonly prescribed antiretroviral drugs (1). Efavirenz pharmacokinetics (PK) is characterized by large interindividual variability in plasma concentrations following a single dose (2, 3) and during chronic administration (4), which has important clinical implications. During the induction phase, efavirenz exposure is associated with central nervous system and psychiatric adverse events, liver enzyme elevation, and rash, among others (5, 6). This may result in increasing rates of

poor adherence and treatment discontinuation or modification (7, 8). The frequency of neuropsychiatric adverse effects is higher during the first days of treatment, and their intensity is greatest in the hours immediately after drug intake, suggesting a relationship with maximum efavirenz concentrations (C_{max}) (9). A recent noninferiority dose-reduction study (ENCORE1) demonstrated that the daily efavirenz dose could be reduced from the standard 600-mg dose to 400 mg without compromising efficacy (6). While there was some evidence of reduced side effects with dose reduction, 37% of patients reported adverse events related to the study drug and the frequency of specific adverse events remained high (6). Therefore, understanding the sources of heterogeneity in drug exposure after initiating efavirenz remains critical to successful therapy, as it impacts both the efficacy and tolerability of the drug.

Variability associated with both absorption and disposition processes likely contribute to efavirenz pharmacokinetic variability. Absolute bioavailability of efavirenz in humans is unknown due to a lack of intravenous formulation, and the extent to which intra- and interindividual variability in bioavailability influence efavirenz exposure is unclear. Administration of efavirenz with food increases the area under the concentration-time curve (AUC) and C_{max} following a single dose and at steady state and increases the frequency of adverse reactions (10, 11). In preclinical studies, high-dose efavirenz was shown to delay gastric emptying (12). If efavirenz similarly affects gastric motility in humans, it may have unpredictable effects on efavirenz exposure and drug interactions. Efavirenz is lipophilic (log of the partition coefficient, ~2.07) (13) and highly bound to plasma proteins (greater than 99%) (14), which may significantly impact its apparent volume of distribution (*V/F*). The apparent volume of distribution of efavirenz has been reported to be larger in females (15, 16), which may be a consequence of altered body composition in females relative to males (17). However, a mechanistic basis for these associations has not been explored.

Hepatic metabolism of efavirenz to form several inactive metabolites is the principal mechanism of efavirenz clearance. Metabolism occurs predominantly through cytochrome P450 (CYP) 2B6-mediated hydroxylation to 8-hydroxy efavirenz, which is further conjugated by glucuronidation and sulfation to form the most abundant plasma metabolites (18, 19). Additional minor primary metabolic pathways include CYP2A6-mediated hydroxylation to form 7-hydroxy efavirenz and formation of efavirenz N-glucuronide by UGT2B7 (20, 21). CYP2B6 also catalyzes the sequential hydroxylation of hydroxylated metabolites to form dihydroxy metabolites (19, 20, 22). Like many of the genes encoding drug-metabolizing enzymes in the human liver, *CYP2B6*, *CYP2A6*, and *UGT2B7* are highly polymorphic (http://www.cypalleles.ki.se/), which contributes to variability in the metabolism of substrates of these enzymes *in vitro* and *in vivo* (23, 24). Of the CYP2B6 alleles studied, *CYP2B6*6* is the most common allele conferring low enzymatic activity, with allele frequencies of 15% to 60% across ethnic groups (24). The *CYP2B6*6* allele codes for two nonsynonymous amino acid changes, Q172H and K262R, with the Q172H substitution conferring reduced function (24).

Efavirenz clearance is significantly reduced in individuals with a *CYP2B6*6/*6* genotype (1.5 to 9-fold relative to the *CYP2B6*1/*1* genotype) following a single dose (2, 3, 15) and at steady state (25–27). Additionally, there are several additional rare *CYP2B6* alleles that confer null or reduced *CYP2B6* activity, resulting in higher efavirenz exposure (28). Intra- and interindividual variability in efavirenz clearance in HIV patients may additionally be influenced by coadministered drugs that are known to induce *CYP2B6* expression and increase *de novo* protein synthesis (16). In contrast with *CYP2B6*, genetic variation in *CYP2A6* and *UGT2B7* has a relatively minor effect on efavirenz clearance, likely due to 7-hydroyxlation and N-glucuronidation being minor elimination pathways (18, 20). However, efavirenz exposure may be increased in individuals harboring reduced-function *CYP2A6* and *UGT2B7* alleles that also have *CYP2B6* poor metabolizer genotypes, though it is unclear whether the exposure change is clinically relevant (29, 30).

A number of population-based pharmacokinetic models have been developed to characterize efavirenz PK in both healthy volunteers and HIV-infected individuals (2, 15,

TABLE 1 Study population demographics and anthropometric measures

Parameter	Median (range) or no.[a]	Mean (SD) or frequency (%)[b]
Age (yr)	24 (18–50)	28 (10)
Wt (kg)	72.7 (53.0–103.6)	74.0 (13.4)
Ht (m)	1.76 (1.55–1.98)	1.75 (0.09)
BMI (kg/m^2)	24.0 (17.8–32.2)	24.2 (3.7)
Fat-free mass (kg)	56.4 (35.6–75.1)	53.7 (10.9)
Fat mass (kg)	18.8 (6.3–42.7)	20.3 (7.2)
Sex		
Male	46	63.0
Female	27	37.0
Race		
Caucasian	52	71.2
African-American	16	21.9
Indian	1	1.4
American Indian	1	1.4
Asian	3	4.1

[a]For all parameters except sex and race, the values are medians (ranges); for sex and race, the values are numbers of participants.
[b]For all parameters except sex and race, the values are means (SDs); for sex and race, the values are frequencies (percent).

25, 27). Many of these studies have focused on genetic determinants of clearance, with a lesser focus on other sources of variability in drug exposure and disposition. Inconsistency between studies as to the covariates evaluated contributes to uncertainty as to their clinical utility in predicting efavirenz PK. These discrepancies may be attributed to many factors: whether the study design was sufficient to address the PK question, focus, and intent of the PK analysis, the availability of covariates, the effects of concomitant medications or disease burden, and therapeutic compliance, among others. We have conducted a population-based pharmacokinetic analysis of intensively sampled plasma efavirenz concentrations in HIV-seronegative volunteers administered a single dose of 600 mg efavirenz. We observed that anthropometric measures of body composition and germ line genetic variation in *CYP2B6* influence both the apparent volume of distribution and clearance of efavirenz.

RESULTS

Study population characteristics. Through an initial telephone screen and baseline physical and clinical laboratory tests, we identified 96 subjects who were eligible for study enrollment. Of these, 73 subjects were enrolled into the study and were orally administered 600 mg efavirenz and the drug cocktail. The remaining 23 eligible subjects could not be enrolled for various reasons (primarily due to failure to report to the Indiana University School of Medicine Clinical Research Center [ICRC] and voluntary dropout). After receiving study drug, three subjects withdrew from the study, of which one withdrawal may have been due to a side effect of efavirenz (the subject reported nausea and vomiting). Baseline characteristics for the study subjects are given in Table 1. Study subjects were young (median age, 25 years; range, 18 to 50 years), and 46 of the 73 subjects were male (63%). The subjects were largely Caucasian (52 of 73; 71.2%) and African-American (16 of 73; 21.9%), with the remaining subjects reporting partial or complete Asian, Indian, or American Indian ancestry (5 of 73; 6.8%). Weight (WT) and body mass index (BMI) were typical of North American populations, and 9 of 73 subjects (12%) were clinically obese (BMI $>$ 30 kg/m^2).

The classification of genetic polymorphisms identified in this study population into expected metabolizer phenotypes is described in Table S1 in the supplemental material. Genetic variants genotyped in this study were those with known functional consequence and occurring at a high frequency in multiple populations. Missing metabolizer phenotypes were a result of technical failures of genotyping one or more variants in the respective genes. Haplotypes could not always be definitively deter-

mined based on the genotyping results. For instance, subjects heterozygous for CYP2B6*4 and CYP2B6*9 variants may have autosomes carrying the *4 and *9 alleles, or the *1 allele and *6 alleles. However, an inability to distinguish haplotypes did not alter the phenotypic classification for most cases.

Population PK model. Our population-based pharmacokinetic analysis of single-dose efavirenz disposition utilized plasma concentration measurements from all 73 subjects enrolled. Of the three subjects that withdrew from the study, blood samples were drawn and plasma efavirenz concentrations were measured in these subjects up to 6, 24, and 48 h after efavirenz administration (a total of 8, 8, and 14 efavirenz concentrations measured, respectively). A single plasma measurement at 6 days (145 h) was available for one subject due to misplaced blood samples prior to efavirenz quantification. Of the remaining 69 subjects, 14 to 16 plasma efavirenz concentrations were measured and analyzed per subject. In total, 1,132 plasma efavirenz concentrations were included from the analysis and two concentrations below the assay lower limit of quantification (LLOQ) were excluded.

A two-compartment model with first-order absorption and a lag time adequately described the data and was used for evaluation of several absorption models. This model included both additive and proportional residual variability terms, and between-subject variability (BSV) in apparent oral clearance was assumed based on exploratory data analysis. Additional BSV random effects were evaluated individually for each model parameter and then added sequentially, resulting in an interim model that included BSV in all model parameters except bioavailability (ΔOFV $= -625$, $P < 0.00001$ [where OFV is objective function value]). Plasma efavirenz concentration profiles in the first 6 h of dosing displayed marked heterogeneity in our study population, suggesting that efavirenz absorption was not uniformly described by first-order absorption kinetics (see Fig. S1 in the supplemental material). Efavirenz absorption was rapid in some individuals, leading to a singular C_{max} following dosing. Other subjects displayed apparent zero-order absorption kinetics resulting in a nearly flat C_{max}, and yet other subjects displayed discontinuous absorption suggestive of different kinetic processes. Apparent double peaks were observed in some subjects, occurring mainly within 6 h of dosing. To better describe efavirenz absorption, we evaluated several empirical models, including first-order absorption processes drawn from bimodal normal distributions estimated using a mixture model, dual simultaneous first-order absorption processes with independent lag times, and sequential or simultaneous zero- and first-order absorption processes with independent lag times. A transit compartment model was also evaluated in which the optimal number of presystemic compartments, the mean transit time to the absorption compartment, and an absorption rate constant were estimated (31). Including BSV for absorption parameters was considered during implementation and comparison of these models. Efavirenz absorption was best described by a simultaneous zero- and first-order absorption model with BSV in the first-order absorption rate constant (K_a), lag times prior to first- and zero-order absorption (t_{lag1} and t_{lag2}), and the duration of the zero-order absorption process (*D2*). We estimated the fraction of the dose administered absorbed through the first-order process ($F1 = 0.414$) and assumed the remainder of the dose was absorbed by zero-order absorption ($F2 = 1 - F1 = 0.586$). While our model did not restrict the order of absorption processes, empirical Bayes estimates of t_{lag1} and t_{lag2} supported a sequential absorption process in most subjects, where absorption initiates with zero-order kinetics and continues as a first-order process ($t_{lag2} = 0.445$ h, $D2 = 0.675$ h, $t_{lag1} = 1.97$ h). The corresponding typical zero-order absorption rate in this study was 1,650,080 nmol/h (521 mg/h). The zero-order process ended prior to initiation of the first-order process in 67 of 73 subjects (92%), with simultaneous absorption processes occurring in the remaining 6 subjects for a median of 0.60 h (range, 0.30 to 1.39 h). Notably, these 6 subjects had absorption profiles characterized by an initial slow zero-order process that correlated with slowly rising plasma concen-

trations in the first 4 h after efavirenz ingestion. Population estimates of absorption parameters were fixed prior to evaluation of covariate effects.

Covariate model development. Investigating covariates that might alter apparent oral clearance (CL/*F*) revealed positive correlation with total body weight (TBW), with similar improvements in OFV when parameterized as a linear (equation 1; ΔOFV = −19.786, $P < 0.05$) or as an allometric relationship (equation 2; ΔOFV = −15.094, $P < 0.05$) (see Materials and Methods for equations). An additional significant relationship between CL/*F* and fat-free mass (FFM) was similarly well described by an allometric model (equation 2; ΔOFV = −19.551, $P < 0.05$) and a linear model (equation 1; ΔOFV = −18.275, $P < 0.05$). Allometric scaling of CL/*F* by normal fat mass (NFM)-suggested fat mass (Ffat = 0.08) has a small contribution to variability in CL/*F* relative to FFM (equation 2; ΔOFV = −16.736, $P < 0.05$; ΔOFV versus FFM alone = 2.815, $P > 0.05$). Further model development accounted for FFM versus WT or NFM given the overall improved fit and mechanistic relationship with clearance. An allometric exponent of 3/4 was fixed in the final model as estimation of the exponent did not significantly lower the overall objective function (ΔOFV = −3.033, $P > 0.05$) and bootstrap estimation did not support an alternative parameterization (mean of 100 bootstrap simulations = 0.72, 95% confidence interval [CI] = 0.60, 0.83). Inclusion of a sex effect on CL/*F* (equation 4) was significant (ΔOFV = −5.138, $P < 0.05$) but did not remain a significant, independent predictor after CL/*F* was adjusted for FFM (ΔOFV = 1.232, $P > 0.05$). Plots showing the relationship between BSV in CL/*F* and fat-free mass for the base and final models are provided in Fig. 1.

We initially identified a correlation between the apparent peripheral volume of distribution (V_p/F) and sex, with females having approximately 20% greater volumes on average (equation 4; ΔOFV = −14.794, $P < 0.05$). Additionally, we observed a significant correlation between V_p/F and BMI that was described by an exponential relationship between BMI and V_p/F (equation 3; ΔOFV = −18.183, $P < 0.05$). After adjustment for BMI, sex remained an independent predictor of volume of distribution (*V*/*F*) (ΔOFV = −7.159, $P < 0.05$). The population-predicted V_p/F in males was approximately 90% of that in females, suggesting that the sex dependency of V_p/F was not fully accounted for after accounting for BMI. A comparison of demographics and anthropometric measures between males and females is provided in Table S2 in the supplemental material. Furthermore, the nonlinear relationship between BMI and V_p/F would extrapolate to extremely large distribution volumes in very obese subjects. Further exploration of the influence of body composition revealed a strong positive relationship between V_p/F and fat mass (FM) that was best described using allometric scaling (equation 2; ΔOFV = −69.202, $P < 0.05$). An allometric exponent of 1 was fixed in the final model as estimation of the exponent resulted in a small improvement in overall model fit (ΔOFV = −4.686, $P < 0.05$) and was not strongly supported by bootstrap estimation (mean of 100 bootstrap simulations = 1.13, 95% CI = 0.79, 1.46). Allometric scaling of V_p/F by FM reduced BSV (% coefficient of variation [%CV]) from 59.1% to 37.4% (Table 2). After accounting for the effect of FM on V_p/F, no other covariates were found to significantly alter V_p/F. Plots showing the relationship between BSV in V_p/F and FM for the base and final models are provided in Fig. 1.

Accounting for FM effect on V_p/F and FFM effects on CL/*F* in the model, stepwise univariate inclusion of metabolizer status for each CYP gene identified CYP2B6 metabolizer status to significantly alter CL/*F* (ΔOFV = −30.164, $P < 0.05$) and reduced BSV (%CV) in CL/*F* from 31.6% to 26.3%. The metabolizer statuses of CYP3A5 (ΔOFV = −11.182, $P < 0.05$), CYP2C8 (ΔOFV = −6.663, $P < 0.05$), and CYP2C19 (ΔOFV = −8.84, $P < 0.05$) were also significant when added individually. However, within each of these models, metabolizer status did not alter CL/*F* by more than 10%, and for CYP3A5 and CYP2C8, there was not a clear trend between metabolizer status and CL/*F*. Furthermore, CYP3A5, CYP2C8, and CYP2C19 metabolizer statuses were not significant in models including metabolizer status of CYP2B6 and were not retained in the final model. Compared to efavirenz CL/*F* of subjects classified as having normal CYP2B6 metabolic

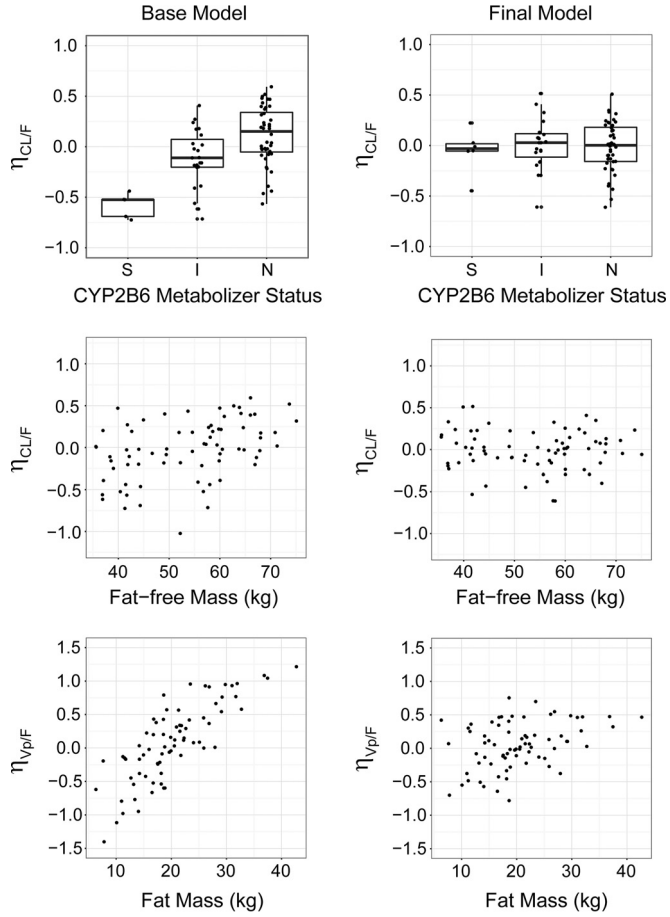

FIG 1 Relationship between CL/*F* or *V*p/*F* and influential covariates for the base and final models. Between-subject variabilities in CL/*F* ($\eta_{CL/F}$) or V_p/F ($\eta_{Vp/F}$) versus CYP2B6 metabolizer status (top panels), fat-free mass (kg) (middle panels), and fat mass (kg) (bottom panels) are shown. These relationships are illustrated for estimates of $\eta_{CL/F}$ and $\eta_{Vp/F}$ prior to incorporation of covariate effects in the model (base model; left column) or after adjusting for these covariates in the model (final model; right column). Boxplots shown in the top panels depict five-number summaries as horizontal lines representing (from top to bottom) 75th percentile + (1.5 × interquartile range) (end of upper whisker), 75th percentile, median, 25th percentile, and 25th percentile − (1.5 × interquartile range) (end of lower whisker).

status, efavirenz CL/*F* was estimated to be reduced by 25% in subjects with reduced CYP2B6 activity (intermediate metabolizer) and to be reduced by 51% in subjects predicted to have slow CYP2B6 metabolic status (*CYP2B6*6/*6*) (Table 2). Estimating CL/*F* for the combined group of CYP2B6 extensive and intermediate metabolizers increased the OFV by 12.879 points ($P > 0.05$), supporting the independent effects of CYP2B6 metabolizer status on efavirenz CL/*F*. No relationships were identified between absorption model parameters and subject demographics or CYP metabolizer status. Plots showing the relationship between BSV in CL/*F* and CYP2B6 metabolizer status for the base and final models are provided in Fig. 1.

After accounting for covariates, model improvement was observed after accounting for correlation between CL/*F* and V_p/F, in addition to correlation between apparent intercompartmental clearance (*Q*/*F*) and *V*p/*F* (ΔOFV = −63.605, $P < 0.05$). Univariate elimination of covariates from the final model resulted in significantly increased OFVs, i.e., +86.947 (CYP2B6 metabolizer status), +14.975 (allometric scaling of FFM on CL/*F*), and + 95.176 (allometric scaling of FM on V_p/F) ($P < 0.0001$), supporting their inclusion in the final model. In summary, the OFV was reduced by 177.084 points after accounting for covariates and parameter correlation. Population parameter estimates for the base and final models given the reference covariate effects (56-kg FFM, 19-kg FM, CYP2B6 normal metabolizer) are summarized in Table 2. As shown in Table 2, fixed and

TABLE 2 Summary of pharmacokinetic parameters

Parameter (unit)[a]	Base model estimate	Final model estimate	Median bootstrap estimate	%RSE[b]
Absorption				
F1	0.414	0.414		
t_{lag1} (h)	1.97	1.97		
K_a (h^{-1})	0.504	0.504		
F2	0.586	0.586		
t_{lag2} (h)	0.445	0.445		
Duration of zero-order absorption (h)	0.675	0.675		
Disposition				
CL/*F* (liters · h^{-1}) (CYP2B6 normal metabolizer; FFM, 56 kg)	6.36	7.52	7.56	1.70
V_c/F (liters)	125	125	127	6.03
V_p/F (liters) (FM, 19 kg)	364	374	386	3.53
Q/F (liters · h^{-1})	37.9	32.3	33.3	5.21
CYP2B6 effect on CL/*F*				
CYP2B6 normal metabolizer (factor)		1		
CYP2B6 reduced metabolizer (factor)		0.752	0.740	5.54
CYP2B6 poor metabolizer (factor)		0.490	0.494	7.22
Between-subject variability (SD)				
CL/*F*	0.366	0.257	0.257	6.85
V_c/F	0.307	0.318	0.318	7.16
V_p/F	0.591	0.374	0.374	7.01
Q/F	0.547	0.671	0.624	15.77
t_{lag1}	0.263	0.271	0.272	7.85
K_a	0.837	0.965	0.952	7.72
t_{lag2}	0.480	0.473	0.472	7.53
Duration of zero-order absorption	0.677	0.703	0.703	6.83
Correlation (ρ)[c]				
CL/*F* to V_p/F		0.196	0.248	59.78
Q/*F* to V_p/F		0.849	0.831	8.27
Residual error				
Proportional error (%)	0.016	0.016	0.130	8.90
Additive error (nmol/liter)	5,290	4,270	4,320	10.78

[a]*F*, bioavailability; *F1*, fraction of dose absorbed by first-order absorption; *F2*, fraction of dose absorbed by zero-order absorption; t_{lag1}, time between dosing event and initiation of first-order absorption from the gut compartment; t_{lag2}, time between dosing event and initiation of zero-order absorption from the gut compartment; duration, duration of time that zero-order absorption occurs following the absorption lag time (t_{lag2}); CL/*F*, apparent oral plasma clearance; V_c/F, apparent central volume of distribution; V_p/F, apparent peripheral volume of distribution; *Q/F*, apparent inter-compartmental clearance; $CL/F = CL_{TV} \times (FFM/56)^{3/4} \times$ factor (liters · h^{-1}) (for subjects with normal CYP2B6 metabolizer status); $V_p/F = V_{p,TV} \times (FM/19)$ (liters). Proportional error, additive error, and between-subject variation are expressed as standard deviations.

[b]Percent relative standard error (%RSE) was calculated from 1,000 bootstrapped parameter estimates. %RSE = 100 × (bootstrap SE/population model parameter estimate).

[c]The correlations between BSV terms *i* and *j* are reported as correlation coefficients, where $\rho_{i,j} = \text{cov}(\omega_i, \omega_j)/(\omega_i \times \omega_j)$.

random-effect parameters were precisely estimated (most with a percent relative standard error [%RSE] of <10%).

Model evaluation. Visual predictive checks (VPCs) resulting from 10,000 simulations from the final model, stratified by CYP2B6 metabolizer status, are shown in Fig. 2. The 5th, 50th, and 95th percentiles of the observed data fell within the respective 95% confidence intervals, indicating that the model described the range of plasma efavirenz concentrations observed following a single dose. Compared to VPCs for CYP2B6 normal and intermediate metabolizers, prediction intervals within the CYP2B6 poor metabolizers were wider, given the limited number of subjects with the *CYP2B6*6/*6* genotypes. A prediction-corrected VPC (pcVPC) provided in Fig. S2 in the supplemental material similarly supports the performance of the final model. The pcVPC suggests underprediction of the 5th and 50th percentiles of plasma concentrations in the early

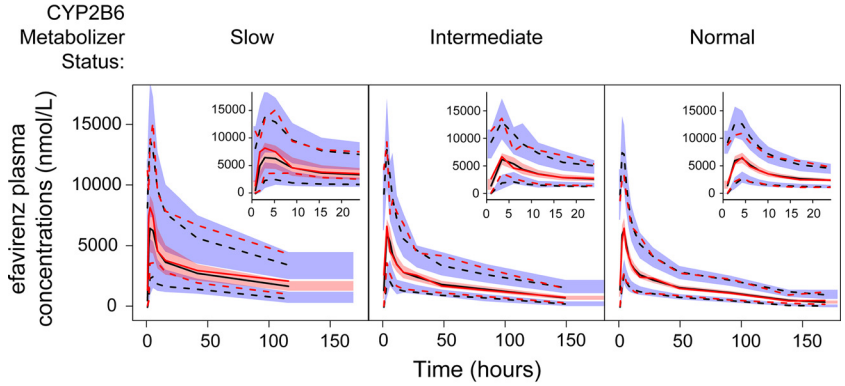

FIG 2 Visual predictive checks of plasma efavirenz concentrations by CYP2B6 metabolizer status. Within each panel, the 95th, median, and 5th percentiles of observed plasma efavirenz concentrations (nmol/liter) within each bin are represented by the upper red dashed line, middle red solid line, and lower red dashed line, respectively. The 95th, median, and 5th percentiles of predicted plasma concentrations (nmol/liter) within each bin are represented by the upper black dashed line, middle black solid line, and lower black dashed line, respectively. The red-shaded area represents the 95% confidence interval for the median predictions, whereas the upper and lower blue-shaded areas represent the 95% confidence intervals for the 95th and 5th percentiles of predicted concentrations, respectively. The inset figures within each panel display the visual predictive checks during the first 24 h after efavirenz administration.

absorption phase, which may be a consequence of median normalizing given the wide range of concentrations observed at these time points. Additional model diagnostic plots are displayed in Fig. 3, which show the goodness of fit of the final PK model to the data. The distribution of conditional weighted residuals was generally uniform across the range of predicted concentrations and time after dose (Fig. 3).

DISCUSSION

Variability in the PK of antiretroviral agents, such as efavirenz, is a well-known determinant of heterogeneity in clinical response and adverse effects (32). Efavirenz

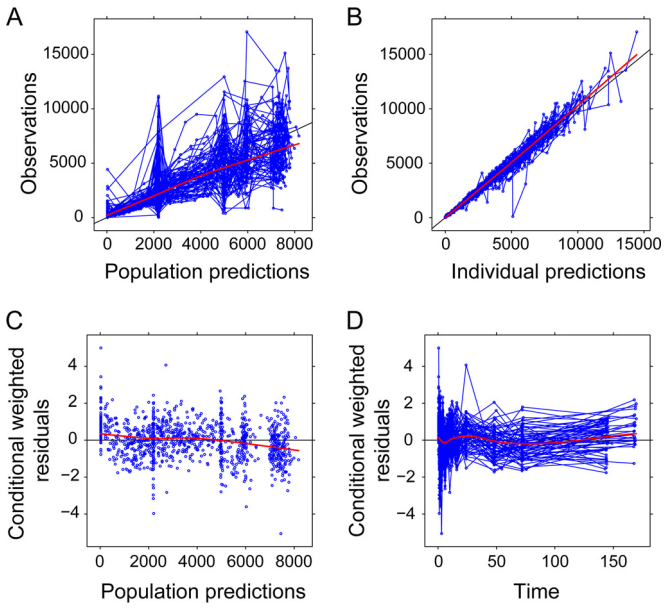

FIG 3 Diagnostic plots for the final population-based pharmacokinetic model. (A and B) Observed plasma efavirenz concentrations (nmol/liter) versus population-predicted (A) or individual-predicted (B) efavirenz concentrations (nmol/liter). Paired observed and predicted concentration measurements for a given subject are plotted as circles and connected by lines. (C) Conditional weighted residuals versus population-predicted efavirenz concentrations (nmol/liter). (D) Conditional weighted residuals versus time (hours). Residuals for a given subject are plotted as circles and connected by lines. In panels A to D, red lines represent the result of a loess smoother with fitting by weighted least-squares.

pharmacokinetic variability has been attributed, in part, to patient characteristics that are variable at a population level (2, 3, 15, 28). Despite this, efavirenz is dosed without regard to patient characteristics. Recent clinical trials support the therapeutic equivalence of 400 mg efavirenz to the historically used dose of 600 mg, citing a similar efficacy and an improved toxicity profile (33). However, these comparisons are largely based on the average response in all trial subjects and individual response may vary widely. Using a population-based pharmacokinetic modeling approach, we have estimated sources and the extent of variability in the absorption, distribution, and elimination of efavirenz following a single oral dose and identified patient factors that markedly influence efavirenz disposition.

The impact of germ line genetic variation on efavirenz clearance has been extensively studied. *In vivo* studies of efavirenz metabolism have largely reflected *in vitro* drug metabolism studies, which show that the primary route of efavirenz elimination is through CYP2B6-mediated hydroxylation (18–20). Of the genetically polymorphic CYPs evaluated in this study, only CYP2B6 metabolizer status was found to be a significant predictor of CL/*F*. Relative to subjects predicted to have normal CYP2B6 metabolizer status, we estimated that CL/*F* is reduced by 25% in subjects with CYP2B6 intermediate metabolizer status (which included a subject with a *1/*18 genotype) and 50% in subjects with poor metabolizer status (*CYP2B6*6/*6* genotypes). Accordingly, BSV in CL/*F* was increased from 25.7% to 35.2% when CYP2B6 metabolizer status was removed from the final model (37% increase in variability). Our results are similar to those of other studies that demonstrate a significant effect of CYP2B6 genotypes on CL/*F* and a 25 to 50% reduction in unexplained BSV upon accounting for *CYP2B6*6* or *CYP2B6* c.516G-to-T alleles (2, 26, 27, 34). It is expected that the *CYP2B6* variants evaluated in this study account for the majority of the influence of *CYP2B6* genetic variability on efavirenz concentrations in the population studied, given the relatively low allelic frequency and/or minor effects of additional variants (28, 35). In addition to *CYP2B6*, *CYP2A6* polymorphisms have been shown to be associated with efavirenz CL/*F*, efavirenz concentrations, or 7-OH efavirenz concentrations (25, 29, 30). In these studies, the relative influence of the *CYP2A6* genotypes on efavirenz PK was more prominent in CYP2B6 slow metabolizers, suggesting that the minor elimination pathway of 7-hydroxylation mediated by CYP2A6 may play an increased role in subjects with low CYP2B6 activity (20). In the present study, CL/*F* was not found to be significantly altered by CYP2A6 metabolizer status when analyzed univariately or in subgroups of CYP2B6 metabolizer status, consistent with our previous findings (2). Our ability to attribute efavirenz concentration changes to a genetic interaction modulating a minor elimination pathway was likely limited by sample size. However, formation of 7-OH efavirenz by CYP2A6 may have a more significant effect on plasma efavirenz concentrations during chronic dosing due to induction of CYP2A6, particularly in those subjects with slow CYP2B6 metabolizer phenotypes who do not exhibit induction of CYP2B6 activity (36–38). Consequently, some gene-gene interactions may be more prominent as efavirenz is dosed to steady state.

In our study, we evaluated the influence of body composition on efavirenz CL/*F* using the traditional scalar weight and compared this to FFM, which has been proposed to approximate the lean tissue mass responsible for drug clearance (17, 39). Given the range of measured body weights and calculated FFM in our study subjects, the relationship between either WT or FFM and CL/*F* was approximately linear. Accordingly, both linear and allometric models provided similar improvements in model fit. Under the assumption that clearance increases linearly with FFM, but nonlinearly with TBW, weight-adjusted clearance may inaccurately predict clearance in obese subjects (39). Therefore, we retained the allometric FFM scalar and suggest that TBW- and FFM-scaled efavirenz clearance be further evaluated over a broader weight range that is biased toward obese subjects. Reported sex differences in efavirenz CL/*F* have been conflicting, with some studies showing associations (3, 40) and others reporting no relationship (15, 16). Similarly, differences in CYP2B6 expression and activity in human liver microsomes between sexes have been inconsistent in the literature (41–43). We observed a

small change in CL/*F* between sexes in this study, with males estimated to have lower clearance (fractional reduction in CL/*F* of <1%); however, this effect was not observed after scaling CL/*F* by FFM. While the contribution of sex to variability in efavirenz clearance cannot be excluded, our results suggest that this effect likely has no clinical significance and may be accounted for by body composition differences between males and females.

As with clearance, there have been contradictory reports regarding the influence of body weight, body composition, and sex on efavirenz distribution. BMI has been reported to be positively correlated with efavirenz V_p/F, inversely correlated with AUC, and uncorrelated with terminal elimination half-life (3). However, other studies have also concluded there is no impact of weight or BMI on V_p/F (27, 44) or did not report whether these effects were considered (15, 25, 40). Weight-normalized apparent volume of distribution has been reported to be 1.6-fold larger in females than males, suggesting that a sex-dependent factor influenced *V*/*F* independent of weight (16). We observed strong associations between sex, BMI, and V_p/F. The median V_p/F of efavirenz was greater in females (507 liters, range = 168 to 1,339 liters) than males (334 liters, range = 76 to 955 liters), and V_p/F increased nonlinearly with BMI. However, subject sex remained a significant predictor of V_p/F after accounting for BMI. Since bioelectrical impedance, a measure of nonconducting adipose tissue, increases linearly with BMI but with a sex-dependent relationship, we hypothesized that the nonlinear but sex-dependent relationship between V_p/F and BMI may be explained by differences in fat composition between sexes (17). We rationalized that differences in body composition between females and males may account for the reported larger weight-normalized apparent volumes of distribution observed in females (3, 16). Exploration of a mechanistic basis for these associations revealed a linear relationship between V_p/F and calculated FM that was well described by allometric scaling. Given the expected lipophilicity of efavirenz, we suspect that these findings have a strong physiologic interpretation. Specifically, our results suggest that the reported associations of sex, weight, and BMI with efavirenz V_p/F reflect distribution and extensive binding of the highly lipophilic drug into tissue compartments with high lipid content, such as adipose. In addition to FM, another determinant of variability in the apparent *V* of efavirenz may be the interaction with plasma proteins. Efavirenz is estimated to be >99% bound to serum albumin, and inter- and intrasubject variability in albumin may contribute to variability in *V*/*F* by modifying plasma/tissue partition (14). Mechanistically, as only free drug is available to diffuse across the membranes and would be available to be enzymatically degraded by the liver, variability in free plasma concentrations may also be an important determinant to variability in efavirenz clearance that is not explained by between-subject differences in enzymatic clearance due to genetic polymorphisms.

The potential impact of fat mass on efavirenz pharmacokinetics and pharmacodynamics (PK/PD) may be complex and counterintuitive. Large distribution volumes are expected to result in longer half-lives and small peak-to-trough changes in plasma concentrations that would be therapeutically favorable. The apparent influence of body composition on drug concentrations would be modified by clearance changes due to subject weight and genetics. However, extensive distribution of drug into adipose tissue, as might occur in extreme obesity, may sufficiently reduce biophase concentrations and increase the probability of viral escape. There are limited studies of the impact of body composition on viral or immunological responses to efavirenz-containing regimens, and we could not identify any cohort study evaluating therapeutic outcomes with respect to measures of body fat composition (45). It has been reported that a morbidly obese patient (BMI, 66 kg/m^2) required dose escalation to 1,800 mg efavirenz once a day to achieve plasma concentrations above 2,000 ng/ml and sufficient suppression of HIV RNA load (46). Further studies are needed to determine the influence of body composition on efavirenz PK/PD, and our results suggest that calculation or measurement of body fat mass may improve the determination of these relationships.

Frequent measurement of plasma concentrations in our study facilitated the inter-

rogation of variability in the absorption and distribution phases of efavirenz disposition, which have been observed (3) but incompletely characterized. Efavirenz concentrations in the absorption and early distribution phases revealed heterogeneous and complex absorption kinetics that were best described by an absorption model with zero- and first-order absorption processes with independent absorption lag times. Our model estimates suggest that zero-order absorption of nearly 60% of the oral efavirenz dose occurs rapidly (absorption duration = 0.675 h, BSV [%CV] = 70.3%) in most subjects following a short lag time (0.445 h, BSV [%CV] = 47.3%) and that the remainder of the dose is absorbed with first-order kinetics following a significant longer absorption lag time of nearly 2 h. Since oral bioavailability is unknown and fixed to 1 in our model, a component of the uncertainty in absorption rates may reflect subject differences in bioavailability. Furthermore, efavirenz has been shown to undergo N-glucuronidation, the product of which may be excreted in the bile and reabsorbed following deconjugation by gut flora (47). Several subjects in this study exhibited secondary peaks beyond the expected end of absorption that would be consistent with enterohepatic recirculation, which was not explicitly modeled in our study. The extent to which enterohepatic recirculation influences the PK of efavirenz is unclear. Our results suggest that the zero-order absorption component largely occurs in the proximal small intestine, with unabsorbed drug undergoing slower absorption later and in lower intestinal regions. These speculations are supported by physiologically based pharmacokinetic modeling of efavirenz absorption, which predicted 40 to 50% of a dose to be absorbed in the duodenum and jejunal segments (48). Additionally, *in vivo* radiopharmacology studies of efavirenz disintegration and gastrointestinal transit time have demonstrated that the average time to 50% gastric emptying of 200- to 300-mg efavirenz tablets administered to fasting healthy volunteers was approximately 30 min (% RSE = 41 to 75%) (49). While we did not explicitly model gastric emptying and intestinal transit, model estimates of time between dosing event and initiation of zero-order absorption from the gut compartment (t_{lag2}), which represent a composite transit rate from the dosing compartment to the site of initial absorption, are consistent with these observed gastric emptying times and suggest that absorption initiates rapidly upon the drug's leaving the stomach. In these studies, there was no apparent correlation between time to disintegration of the efavirenz and its PK, suggesting that the rate and extent of dissolution may be a significant contributor to variability in efavirenz absorption kinetics (49). Under these conditions, the low aqueous solubility of efavirenz may limit absorption, and patient variability in water content, native surfactants, and coingested food or medications, among other factors, may influence the rate and extent of absorption during intestinal transit (50, 51). Consistent with our observations, sequential zero- and first-order absorption models have best described the absorption of other compounds with suspected dissolution-limited absorption (52, 53). Dissolution-limited absorption of efavirenz may account for the reported nondose proportionality of C_{max} for oral doses ranging from 100 to 1,600 mg (11).

Understanding variability in efavirenz absorption and identifying factors that describe BSV in the rate, duration, and extent of absorption may provide additional guidance to limit adverse effects. Higher efavirenz concentrations are associated with acute neuropsychiatric disorders during the induction phase and during chronic therapy (54, 55). While acute central nervous system side effects may be transient in some patients, over one-third of patients have side effects that persist during chronic therapy, which are significantly associated with plasma drug concentrations (55, 56). For side effects that exhibit a direct correlation to plasma concentrations, we would expect factors contributing to variability in C_{max} to significantly impact a patient's risk. Current adult dosing recommendations for efavirenz account for the known effect of food to increase efavirenz C_{max} and neuropsychiatric side effects (11).

Limitations. Due to the significant food effect on efavirenz absorption, efavirenz-containing regimens are prescribed to be taken at bedtime, several hours following an evening meal (11). While subjects in our study were instructed to fast overnight prior

to drug administration, actual food intake was unmonitored. Given the ability of moderate- and high-fat diets to increase efavirenz absorption, food effects cannot be ruled out as a source of variability in absorption or bioavailability. We also expect additional imprecision in PK parameter estimates due to an incomplete understanding of the extent of efavirenz bioavailability, which was fixed to 1 in our analysis.

An additional potential limitation was the use of calculated estimates of fat mass and fat-free mass based on semimechanistic models derived by Janmahasatian et al., who utilized volunteers from Brisbane, Australia (17). Racial differences in body composition have been shown for fat-free body mass and fat patterning (57). It is unclear how potential racial differences between populations might influence the generalizability of models to predicted fat-free mass and, by extension, the correlation between body composition and efavirenz disposition identified in this study. Utilizing direct measures of body composition (e.g., bioelectrical impedance analysis [BIA] or dual-energy X-ray absorptiometry [DXA]) in future studies of efavirenz PK would be expected to more precisely estimate these relationships, independent of potential confounders like race. While our study population had a broad distribution of body composition (Table 1), it included few obese (BMI $>$ 30 kg/m^2) and no morbidly obese (BMI $>$ 40 kg/m^2) patients. Therefore, extrapolation of the relationship between *V/F* and FM should be done cautiously in subjects with very high FM before these relationships are independently confirmed.

Our study did not evaluate the potential influence of genetic variation in *UGT2B7* on efavirenz disposition. However, N-glucuronidation is likely a minor pathway of efavirenz clearance, as evidenced by the low plasma concentrations of conjugated efavirenz relative to other metabolites and the small amount of conjugated efavirenz excreted in the urine following a single oral dose of 600 mg (47).

Summary. Using population-based pharmacokinetic analysis, we have developed a model that accounts for subject genotype-predicted CYP2B6 metabolizer status and body composition to estimate plasma efavirenz concentrations following a single dose. This model provides a framework to mechanistically account for the influence of patient-specific factors, such as genetics, sex, weight, and obesity. Our findings may have relevance to dosing efavirenz in obese patients.

MATERIALS AND METHODS

Study subjects. Subjects were recruited between August 2007 and April 2010. The study protocol was approved by the Indiana University Institutional Review Board and conducted at the Indiana University School of Medicine Clinical Research Center (ICRC). Subjects were male and female volunteers, ages 18 to 49 years, free of significant medical conditions. Subjects must have been nonsmokers or willing to refrain from smoking or the use of tobacco or marijuana for at least 1 month prior to and until the completion of the study. Upon enrollment in the study, individuals must have adhered to the study dietary restrictions. After written informed consent was obtained, subjects completed a thorough medical history, physical examination, and laboratory tests, including electrocardiography (EKG), HIV test, urinalysis, and blood tests (complete blood count [CBC], complete metabolic panel, and urine pregnancy tests for females). Females with a positive pregnancy test before and at any time during the study were excluded or participation was discontinued. At this time, venous blood was also drawn for DNA isolation, and demographic characteristics such as body weight, height, sex, race, or ethnic background were collected. Detailed dietary restrictions and inclusion and exclusion criteria have been previously reported and are outlined in the text in the supplemental material (58, 59). The trial was registered at Clinical Trials.gov (http://www.clinicaltrials.gov) under identifier no. NCT00668395.

Study design. This open label study was conducted to evaluate efavirenz PK, pharmacogenetics, and drug interactions after single and multiple doses of efavirenz. Here, we present data that relate to the PK of a single 600-mg oral dose of efavirenz. Efavirenz PK following a single oral dose was measured during a 24-h inpatient stay, followed by 3 outpatient visits over 6 days. On day 1, subjects were requested to arrive in the morning (~8 a.m.) in the ICRC after overnight fasting. Vital signs and EKGs were obtained for all subjects, and female subjects were confirmed to be nonpregnant by a urine pregnancy test. An indwelling intravenous catheter was placed in an arm vein, and a predose (baseline) blood draw was obtained. The subjects were then administered a single oral dose of efavirenz (Sustiva [Bristol-Myers Squibb]; 600-mg tablet) with 240 ml water. One hour later, an oral drug cocktail (250 mg tolbutamide, 20 mg omeprazole, 150 mg caffeine, and 1 mg of midazolam syrup) was administered with water. Blood samples (10 ml) were scheduled to be collected 0.5, 1, 1.5, 2, 2.5, 3, 4, 6, 8, 10, 12, 16, and 24 h after efavirenz dosing. Plasma was separated by centrifugation within an hour of collection and immediately stored at −80°C. Vital signs and an EKG were measured every 6 h during the 24-h inpatient stay at the ICRC. Also, blood sugar was measured 0.5 h after tolbutamide administration and monitored if subjects

exhibited low blood sugar. On subsequent days, additional venous blood samples were scheduled to be collected at the ICRC (often in the morning) at 48, 72, and 144 h after efavirenz dosing.

Measurement of efavirenz and its metabolites. Plasma concentrations of efavirenz and its metabolites were determined after enzymatic deconjugation. Plasma samples (250 μl) were mixed with 250 μl of 0.2 M sodium acetate (pH 5), 12.5 μl of 600 mM sodium azide, and 25 μl of β-glucuronidase (1,000 U/ml) and then incubated at 37°C for 18 h on a shaker. After deconjugation, the internal standards (30 μl of 1 μg/ml efavirenz-d4, 1 μg/ml chloropropamide, 1 μg/ml triazolam, and 1 μg/ml acetaminophen) were added and extracted with 250 μl of 0.1 M hydrochloric acid and 6 ml of ethyl acetate-hexane (50:50, vol/vol). After shaking for 10 min and centrifugation at 3,600 rpm for 10 min (0°C), the organic layer was removed and evaporated to dryness. The residue was reconstituted in 120 μl of mobile phase A:B (50:50, vol/vol) from which 25 μl was injected onto the high-performance liquid chromatography–tandem mass spectrometry (HPLC-MS/MS) system.

Analysis was performed on an API 3200 triple-quadrupole mass spectrometer (Applied Biosystem/AB Sciex, Foster City, CA) equipped with a turbo ion spray source. The HPLC system consisted of two LC-20AD pumps, an SIL-20AHT UFLC autosampler, a DGU-20A3 degasser, and a CBM-20A controller (Shimadzu, Columbia, MD). Chromatographic separation was performed on a C_8 column (250 by 4.6 mm, 5-μm particle size; Restek, Bellefonte, PA). Before and after each injection, the needle was washed with acetonitrile-water (75:25, vol/vol). Chromatographic separation was performed using mobile phase A (methanol–0.1% formic acid; 1:99, vol/vol) and mobile phase B (methanol–0.1% formic acid; 99:1, vol/vol) delivered at 0.8 ml/min using a linear gradient of 25% B to 90% B between 0.01 min and 16 min, followed by reequilibration to initial conditions between 16.01 min and 20.00 min. MS optimization was achieved via adjustment of both the compound-dependent and instrument-dependent parameters for efavirenz, 8-hydroxyefavirenz (8-OH EFV), 7-hydroxyefavirenz (7-OH EFV), and 8,14-dihydroxyefavirenz (8,14-diOH EFV) in negative mode using efavirenz-d4 as an internal standard. The analytes were optimized at a source temperature of 550°C in negative mode, under unit resolution for quadrupoles 1 and 3, and were given a dwell time of 60 ms and a setting time of 700 ms. Optimal gas pressures for all analytes, including the internal standards in negative mode, were as follows: collision gas, 8 lb/in^2; curtain gas, 20 lb/in^2; ion source gas 1, 55 lb/in^2; ion source gas 2, 45 lb/in^2; and ion spray voltage, −3,000 V. Multiple-reaction monitoring at *m/z* of 313.97/244.01, 329.98/210.0, 329.98/257.89, 345.91/262.0, and 318.01/247.95 was used to measure first and third quadrupole (Q1/Q3) transitions for efavirenz, 8-hydroxyefavirenz, 7-hydroxyefavirenz, 8,14-dihydroxyefavirenz, and efavirenz-d4, respectively, in negative mode. Data acquisition and processing were performed using Analyst software. The upper and lower limits of efavirenz quantification were 1,000 ng/ml and 1 ng/ml, respectively, with intraday and interday variabilities of <10% and <20%, respectively.

DNA genotyping. Genomic DNA was extracted from whole blood with a DNA minikit (Qiagen, Valencia, CA). Genotyping for variants of the CYP genes were performed using two platforms: TaqMan assay reagent allelic discrimination kits according to the supplier's instructions (Applied Biosystems, Foster City, CA) as previously described (58) and/or the OpenArray platform (Applied Biosystems, Inc., Foster City, CA). The following variants were assayed: *CYP2B6*2* (rs8192709), *CYP2B6*4* (rs2279343), *CYP2B6*5* (rs3211371), *CYP2B6*9* (rs3745274), *CYP2B6*16* (rs28399499), *CYP2B6*18* (rs28399499); *CYP2A6*2* (rs1801272), *CYP2A6*9* (rs8192726), *CYP2A6*12* (rs4803380); *CYP2C8*2* (rs11572103), *CYP2C8*3* (rs11572080, rs10509681); *CYP2C9*2* (rs1799853), *CYP2C9*3* (rs1057910); *CYP2C19*2* (rs4244285), *CYP2C19*3* (rs4986893), *CYP2C19*17* (rs12248560); *CYP3A4* (rs2246709), *CYP3A4* (rs35599367); *CYP3A5*3* (rs776746), *CYP3A5*6* (rs10264272), and *CYP3A5*7* (rs41303343). The *CYP2B6*6* allele consists of the *CYP2B6*4* (G-to-A) and *CYP2B6*9* (T-to-A) variants on the same haplotype.

CYP nomenclature and predicted metabolizer status. Star alleles of CYP genes were designated from the genotyping data in accordance with the Human Cytochrome P450 Allele Nomenclature Database (http://www.cypalleles.ki.se/). The functional consequence of individual *CYP2B6* star alleles was defined based on the reported impact on *in vitro* metabolism of efavirenz and/or changes in efavirenz PK (28, 35, 41), whereas the functional status of star alleles of the other CYP genes was determined based on a consensus of known alterations in metabolism or PK of other selective substrates. For each CYP, genotype-predicted categorical phenotypes were determined (e.g., ultrarapid, normal, intermediate, or slow), and subjects were classified based on their number of reduced-function star alleles.

Population pharmacokinetic modeling. Population pharmacokinetic modeling was performed using the first-order conditional estimation method with interaction (FOCE-I) implemented in NONMEM 7.3 (60). NONMEM was utilized with the Wings for NONMEM package (version 7) (61), Perl-speaks-NONMEM (version 4.4.8) (62), Xpose (version 4) (63), and Pirana (version 2.9.4) (63). Data manipulation and graphical analysis were performed using R (version 3.2.5) (64). Plasma concentrations were fit on a linear scale, and concentrations below the lower limit of quantification (LLOQ) were excluded from model evaluation because they comprised only 2 of the 1,132 plasma concentrations measured.

Pharmaco-statistical model development. (i) Base model development. The compartmental model structure was developed through sequential evaluation of one, two, and three compartments, with first-order absorption and first-order elimination from the central compartment. Efavirenz bioavailability in humans is unknown due to a lack of intravenous formulation and was assumed to be 1 with no interindividual variability. Pharmacokinetic parameters (θ_i) were assumed to be log-normally distributed with between-subject variability (BSV; ω_i) estimated as normally distributed with mean zero and standard deviation of η_i [$\omega \sim N(0,\eta)$]. Residual variability was modeled by considering additive and proportional error terms individually and in combination. Several oral absorption models were evaluated to describe the observed heterogeneity in absorption profiles, with both rapid and delayed profiles. To

avoid overparameterization, error models were refined though stepwise elimination of random effects for individual PK parameters.

(ii) Covariate model development. Following development of the base model, we evaluated whether covariates explained and therefore reduced the unexplained intersubject variability in model parameters. Observed (baseline total body weight, baseline height) and calculated (body mass index, fat-free mass, fat mass) measures of body size and composition were evaluated, along with sex, age, and ethnicity, for their influence on apparent oral clearance and apparent volume of distribution. We additionally determined whether metabolizer status for *CYP2B6*, *CYP2A6*, *CYP2C8*, *CYP2C9*, *CYP2C19*, *CYP3A4*, and *CYP3A5* explained BSV in apparent oral clearance. *CYP2B6*, *CYP2A6*, *CYP3A4*, and *CYP3A5* have been shown to contribute to efavirenz metabolism *in vitro* (19, 20) and were the primary genetic covariates of interest, whereas *CYP2C8*, *CYP2C9*, and *CYP2C19* were genotyped due to their effects on the drug cocktail administered and thus served as negative controls. The fat-free mass (FFM; kg) of each subject was estimated using total body weight (TBW; kg), height, and sex, as described by Janmahasatian et al., and then the fat mass (FM; kg) was then calculated as the difference between TBW and calculated FFM content (FM = TBW − FFM) (17). Additionally, normal fat mass (NFM; kg) was estimated to determine the separate contributions of FM and FFM to the prediction of oral clearance [NFM = FFM + Ffat × (TBW − FFM) (65). The estimated parameter Ffat accounts for the additional contribution of FM versus FFM. Covariate selection was guided by observed covariate relationships between model parameter random effects and/or empirical Bayes parameter estimates; covariates with known or suspected influence on PK parameters were specifically evaluated.

The influence of weight and body composition on disposition parameters was based on either linear relationships of a centered covariate (equation 1) or allometric theory (equation 2) (66, 67):

$$\mathrm{P} = \mathrm{P_{TV}} + \theta\left(\mathrm{size}_i - \mathrm{size_{ref}}\right) \tag{1}$$

$$\mathrm{P} = \mathrm{P_{TV}} \times \left(\frac{\mathrm{size}_i}{\mathrm{size_{ref}}}\right)^{\mathrm{exp}} \tag{2}$$

where P is the population PK parameter estimate for a subject(s) with size *i*, P_{TV} is the population estimate for a subject with the reference size ($size_{ref}$), θ is the slope of the relationship between the centered covariate and P, and exp is the allometric exponent, initially assumed to be 3/4 for apparent oral clearance and 1 for the apparent volume of distribution. We additionally evaluated whether the data supported alternative parameterization of allometric exponents (exp) by estimating parameter confidence intervals (CIs) using bootstrap estimates. Exponents were fixed to the value assumed *a priori* if this value fell within the bootstrap-estimated CIs.

A nonlinear centered model was evaluated to approximate the relationship between body mass index (BMI) and apparent peripheral volume of distribution (V_p) (equation 3):

$$V_{\mathrm{p}} = V_{\mathrm{p,TV}} + e^{\theta \times (\mathrm{BMI} - \mathrm{BMI_{ref}})} \tag{3}$$

Binary categorical covariates (COVs) were coded as (0, 1) and evaluated using power (equation 4) and independent (equation 5) models:

$$\mathrm{P} = \theta_0\, \theta_1^{\mathrm{cov}} \tag{4}$$

$$\mathrm{IF}\left(\mathrm{COV} = 0\right)\ \mathrm{P} = \theta_0\ \mathrm{ELSE}\ \mathrm{P} = \theta_1 \tag{5}$$

where the population parameter estimate (P) equals θ_0 when the COV is 0 and $\theta_0\theta_1$ or θ_1 when the COV is 1 (for equations 4 and 5, respectively). The independent model (equation 5) was used to evaluate parameterization of different random effects among covariate groups. Gene-dose effects of CYP metabolizer scores were evaluated using an extended power model (equation 6):

$$\mathrm{P} = \mathrm{P_{TV}} \times \sum_{i=0}^{j-1} \theta_i^{\mathrm{GENO}_i} \tag{6}$$

where P_{TV} represents the parameter estimate for subjects with normal metabolizer scores and *j* is the number of metabolizer score groups (0,1,. . .,*j*). $GENO_i$ is an indicator variable that takes the value of 1 for subjects assigned the i^{th} genotype score (e.g., $GENO_0$ equals 1 for slow metabolizer status, and $GENO_1$ equals 1 for intermediate metabolizer status) and 0 otherwise. The equation 6 model was extended to evaluate the joint influence of CYP2B6 and CYP2A6 metabolizer status, where P_{TV} represents parameter estimates for subjects assigned CYP2B6 and CYP2A6 normal metabolizer status, and $GENO_i$ takes the value of 1 for each additional CYP2B6-CYP2A6 genotype combination and 0 otherwise. Combining CYP metabolizer scores (e.g., P_{TV} represents parameter estimates for subjects assigned intermediate or normal metabolizer status and $GENO_0$ equals 1 for slow metabolizer status) was compared with estimating separate fixed effects for each score level by comparing objective function value (OFV) changes between equations 6 and 7:

$$\mathrm{P} = \mathrm{P_{TV}} \times \sum_{i=0}^{j-2} \theta_i^{\mathrm{GENO}_i} \tag{7}$$

Model evaluation and selection were guided by the following: (i) a decrease in the OFV between two hierarchical models of at least 3.84 (α = 0.05, 1 df) or 5.99 (α = 0.05, 2 df), (ii) visual predictive checks (VPCs), (iii) investigation of weighted residuals, and (iv) visual inspection of the fit between predicted and observed individual concentration-time profiles. In addition, (v) elimination of trends in the relationship between covariates and random-effect estimates and (vi) reduction in the magnitude of random effects

were considered during covariate evaluation. Bin selection for VPC diagnostics was guided using the automatic binning algorithm implemented in Perl-speaks-NONMEM.

SUPPLEMENTAL MATERIAL

Supplemental material for this article may be found at https://doi.org/10.1128/AAC.01813-16.

TEXT S1, PDF file, 0.2 MB.

ACKNOWLEDGMENTS

We thank the participating subjects.

The authors have no conflicts of interest to declare.

This project was supported by award number R01GM078501, 3R01GM078501-04S1, R56 grant 2R56GM067308-09A1, and 5T32-GM008425 from the National Institute of General Medical Sciences, National Institutes of Health (Bethesda, MD), and by award number M01-RR00750 from the National Center for Research Resources (NCRR), a component of the National Institutes of Health (NIH).

J.D.R., Z.D., and R.R.B. contributed to the manuscript writing. J.D.R., Z.D., and R.R.B. analyzed and interpreted data. Z.D., I.F.M., and N.T. coordinated the clinical study. Z.D. designed the research study, and all authors performed the research.

REFERENCES

1. World Health Organization. November 2015. Consolidated guidelines on the use of antiretroviral drugs for treating and preventing HIV infection: what's new. http://www.who.int/hiv/pub/arv/policy-brief-arv-2015/en/. Accessed 25 April 2016.
2. Abdelhady AM, Desta Z, Jiang F, Yeo CW, Shin JG, Overholser BR. 2014. Population pharmacogenetic-based pharmacokinetic modeling of efavirenz, 7-hydroxy- and 8-hydroxyefavirenz. J Clin Pharmacol 54:87–96. https://doi.org/10.1002/jcph.208.
3. Haas DW, Gebretsadik T, Mayo G, Menon UN, Acosta EP, Shintani A, Floyd M, Stein CM, Wilkinson GR. 2009. Associations between CYP2B6 polymorphisms and pharmacokinetics after a single dose of nevirapine or efavirenz in African americans. J Infect Dis 199:872–880. https://doi.org/10.1086/597125.
4. Kappelhoff BS, Huitema AD, Yalvac Z, Prins JM, Mulder JW, Meenhorst PL, Beijnen JH. 2005. Population pharmacokinetics of efavirenz in an unselected cohort of HIV-1-infected individuals. Clin Pharmacokinet 44:849–861. https://doi.org/10.2165/00003088-200544080-00006.
5. Kappelhoff BS, van Leth F, Robinson PA, MacGregor TR, Baraldi E, Montella F, Uip DE, Thompson MA, Russell DB, Lange JM, Beijnen JH, Huitema AD, 2NN Study Group. 2005. Are adverse events of nevirapine and efavirenz related to plasma concentrations? Antivir Ther 10:489–498.
6. ENCORE1 Study Group ES, Puls R, Amin J, Losso M, Phanuphak P, Nwizu C, Orrell C, Young B, Shahar E, Wolff M, Gazzard B, Read T, Hill A, Cooper DA, Emery S. 2014. Efficacy of 400 mg efavirenz versus standard 600 mg dose in HIV-infected, antiretroviral-naive adults (ENCORE1): a randomised, double-blind, placebo-controlled, non-inferiority trial. Lancet 383:1474–1482. https://doi.org/10.1016/S0140-6736(13)62187-X.
7. Leutscher PD, Stecher C, Storgaard M, Larsen CS. 2013. Discontinuation of efavirenz therapy in HIV patients due to neuropsychiatric adverse effects. Scand J Infect Dis 45:645–651. https://doi.org/10.3109/00365548.2013.773067.
8. Elzi L, Marzolini C, Furrer H, Ledergerber B, Cavassini M, Hirschel B, Vernazza P, Bernasconi E, Weber R, Battegay M, Swiss HIV Cohort Study. 2010. Treatment modification in human immunodeficiency virus-infected individuals starting combination antiretroviral therapy between 2005 and 2008. Arch Intern Med 170:57–65. https://doi.org/10.1001/archinternmed.2009.432.
9. European Medicines Agency. 30 March 2016. Sustiva: summary of product characteristics. http://www.ema.europa.eu/docs/en_GB/document_library/EPAR_-_Product_Information/human/000249/WC500058311.pdf. Accessed 5 August 2016.
10. Lamorde M, Byakika-Kibwika P, Tamale WS, Kiweewa F, Ryan M, Amara A, Tjia J, Back D, Khoo S, Boffito M, Kityo C, Merry C. 2012. Effect of food on the steady-state pharmacokinetics of tenofovir and emtricitabine plus efavirenz in Ugandan adults. AIDS Res Treat 2012:105980. https://doi.org/10.1155/2012/105980.
11. Bristol-Myers Squibb Company. 2016. Sustiva® (efavirenz) capsules and tablets. Full prescribing information. Bristol-Myers Squibb Company, New York, NY. http://packageinserts.bms.com/pi/pi_sustiva.pdf. Accessed 5 August 2016.
12. Balani SK, Kauffman LR, deLuna FA, Lin JH. 1999. Nonlinear pharmacokinetics of efavirenz (DMP-266), a potent HIV-1 reverse transcriptase inhibitor, in rats and monkeys. Drug Metab Dispos 27:41–45.
13. Almond LM, Hoggard PG, Edirisinghe D, Khoo SH, Back DJ. 2005. Intracellular and plasma pharmacokinetics of efavirenz in HIV-infected individuals. J Antimicrob Chemother 56:738–744. https://doi.org/10.1093/jac/dki308.
14. Avery LB, Sacktor N, McArthur JC, Hendrix CW. 2013. Protein-free efavirenz concentrations in cerebrospinal fluid and blood plasma are equivalent: applying the law of mass action to predict protein-free drug concentration. Antimicrob Agents Chemother 57:1409–1414. https://doi.org/10.1128/AAC.02329-12.
15. Mukonzo JK, Roshammar D, Waako P, Andersson M, Fukasawa T, Milani L, Svensson JO, Ogwal-Okeng J, Gustafsson LL, Aklillu E. 2009. A novel polymorphism in ABCB1 gene, CYP2B6*6 and sex predict single-dose efavirenz population pharmacokinetics in Ugandans. Br J Clin Pharmacol 68:690–699. https://doi.org/10.1111/j.1365-2125.2009.03516.x.
16. Cho DY, Shen JH, Lemler SM, Skaar TC, Li L, Blievernicht J, Zanger UM, Kim KB, Shin JG, Flockhart DA, Desta Z. 2016. Rifampin enhances cytochrome P450 (CYP) 2B6-mediated efavirenz 8-hydroxylation in healthy volunteers. Drug Metab Pharmacokinet 31:107–116. https://doi.org/10.1016/j.dmpk.2015.07.002.
17. Janmahasatian S, Duffull SB, Ash S, Ward LC, Byrne NM, Green B. 2005. Quantification of lean bodyweight. Clin Pharmacokinet 44:1051–1065. https://doi.org/10.2165/00003088-200544100-00004.
18. Aouri M, Barcelo C, Ternon B, Cavassini M, Anagnostopoulos A, Yerly S, Hugues H, Vernazza P, Gunthard HF, Buclin T, Telenti A, Rotger M, Decosterd LA, Swiss HIV Cohort Study. 2016. In vivo profiling and distribution of known and novel phase I and phase II metabolites of efavirenz in plasma, urine, and cerebrospinal fluid. Drug Metab Dispos 44:151–161. https://doi.org/10.1124/dmd.115.065839.
19. Ward BA, Gorski JC, Jones DR, Hall SD, Flockhart DA, Desta Z. 2003. The cytochrome P450 2B6 (CYP2B6) is the main catalyst of efavirenz primary and secondary metabolism: implication for HIV/AIDS therapy and utility of efavirenz as a substrate marker of CYP2B6 catalytic activity. J Pharmacol Exp Ther 306:287–300. https://doi.org/10.1124/jpet.103.049601.
20. Ogburn ET, Jones DR, Masters AR, Xu C, Guo Y, Desta Z. 2010. Efavirenz primary and secondary metabolism in vitro and in vivo: identification of novel metabolic pathways and cytochrome P450 2A6 as the principal

catalyst of efavirenz 7-hydroxylation. Drug Metab Dispos 38:1218–1229. https://doi.org/10.1124/dmd.109.031393.
21. Belanger AS, Caron P, Harvey M, Zimmerman PA, Mehlotra RK, Guillemette C. 2009. Glucuronidation of the antiretroviral drug efavirenz by UGT2B7 and an in vitro investigation of drug-drug interaction with zidovudine. Drug Metab Dispos 37:1793–1796. https://doi.org/10.1124/dmd.109.027706.
22. Mutlib AE, Chen H, Nemeth GA, Markwalder JA, Seitz SP, Gan LS, Christ DD. 1999. Identification and characterization of efavirenz metabolites by liquid chromatography/mass spectrometry and high field NMR: species differences in the metabolism of efavirenz. Drug Metab Dispos 27:1319–1333.
23. McDonagh EM, Wassenaar C, David SP, Tyndale RF, Altman RB, Whirl-Carrillo M, Klein TE. 2012. PharmGKB summary: very important pharmacogene information for cytochrome P-450, family 2, subfamily A, polypeptide 6. Pharmacogenet Genomics 22:695–708. https://doi.org/10.1097/FPC.0b013e3283540217.
24. Zanger UM, Klein K. 2013. Pharmacogenetics of cytochrome P450 2B6 (CYP2B6): advances on polymorphisms, mechanisms, and clinical relevance. Front Genet 4:24. https://doi.org/10.3389/fgene.2013.00024.
25. Arab-Alameddine M, Di Iulio J, Buclin T, Rotger M, Lubomirov R, Cavassini M, Fayet A, Decosterd LA, Eap CB, Biollaz J, Telenti A, Csajka C, Swiss HIV Cohort Study. 2009. Pharmacogenetics-based population pharmacokinetic analysis of efavirenz in HIV-1-infected individuals. Clin Pharmacol Ther 85:485–494. https://doi.org/10.1038/clpt.2008.271.
26. Cabrera SE, Santos D, Valverde MP, Dominguez-Gil A, Gonzalez F, Luna G, Garcia MJ. 2009. Influence of the cytochrome P450 2B6 genotype on population pharmacokinetics of efavirenz in human immunodeficiency virus patients. Antimicrob Agents Chemother 53:2791–2798. https://doi.org/10.1128/AAC.01537-08.
27. Sanchez A, Cabrera S, Santos D, Valverde MP, Fuertes A, Dominguez-Gil A, Garcia MJ, Tormes G. 2011. Population pharmacokinetic/pharmacogenetic model for optimization of efavirenz therapy in Caucasian HIV-infected patients. Antimicrob Agents Chemother 55:5314–5324. https://doi.org/10.1128/AAC.00194-11.
28. Rotger M, Tegude H, Colombo S, Cavassini M, Furrer H, Decosterd L, Blievernicht J, Saussele T, Gunthard HF, Schwab M, Eichelbaum M, Telenti A, Zanger UM. 2007. Predictive value of known and novel alleles of CYP2B6 for efavirenz plasma concentrations in HIV-infected individuals. Clin Pharmacol Ther 81:557–566. https://doi.org/10.1038/sj.clpt.6100072.
29. di Iulio J, Fayet A, Arab-Alameddine M, Rotger M, Lubomirov R, Cavassini M, Furrer H, Gunthard HF, Colombo S, Csajka C, Eap CB, Decosterd LA, Telenti A, Swiss HIV Cohort Study. 2009. In vivo analysis of efavirenz metabolism in individuals with impaired CYP2A6 function. Pharmacogenet Genomics 19:300–309. https://doi.org/10.1097/FPC.0b013e328328d577.
30. Haas DW, Kwara A, Richardson DM, Baker P, Papageorgiou I, Acosta EP, Morse GD, Court MH. 2014. Secondary metabolism pathway polymorphisms and plasma efavirenz concentrations in HIV-infected adults with CYP2B6 slow metabolizer genotypes. J Antimicrob Chemother 69:2175–2182. https://doi.org/10.1093/jac/dku110.
31. Savic RM, Jonker DM, Kerbusch T, Karlsson MO. 2007. Implementation of a transit compartment model for describing drug absorption in pharmacokinetic studies. J Pharmacokinet Pharmacodyn 34:711–726. https://doi.org/10.1007/s10928-007-9066-0.
32. Marzolini C, Telenti A, Decosterd LA, Greub G, Biollaz J, Buclin T. 2001. Efavirenz plasma levels can predict treatment failure and central nervous system side effects in HIV-1-infected patients. AIDS 15:71–75. https://doi.org/10.1097/00002030-200101050-00011.
33. ENCORE1 Study Group, Carey D, Puls R, Amin J, Losso M, Phanupak P, Foulkes S, Mohapi L, Crabtree-Ramirez B, Jessen H, Kumar S, Winston A, Lee MP, Belloso W, Cooper DA, Emery S. 2015. Efficacy and safety of efavirenz 400 mg daily versus 600 mg daily: 96-week data from the randomised, double-blind, placebo-controlled, non-inferiority ENCORE1 study. Lancet Infect Dis 15:793–802. https://doi.org/10.1016/S1473-3099(15)70060-5.
34. Salem AH, Fletcher CV, Brundage RC. 2014. Pharmacometric characterization of efavirenz developmental pharmacokinetics and pharmacogenetics in HIV-infected children. Antimicrob Agents Chemother 58:136–143. https://doi.org/10.1128/AAC.01738-13.
35. Swart M, Evans J, Skelton M, Castel S, Wiesner L, Smith PJ, Dandara C. 2015. An expanded analysis of pharmacogenetics determinants of efavirenz response that includes 3′-UTR single nucleotide polymorphisms among Black South African HIV/AIDS patients. Front Genet 6:356. https://doi.org/10.3389/fgene.2015.00356.
36. Itoh M, Nakajima M, Higashi E, Yoshida R, Nagata K, Yamazoe Y, Yokoi T. 2006. Induction of human CYP2A6 is mediated by the pregnane X receptor with peroxisome proliferator-activated receptor-gamma coactivator 1alpha. J Pharmacol Exp Ther 319:693–702. https://doi.org/10.1124/jpet.106.107573.
37. Ngaimisi E, Mugusi S, Minzi O, Sasi P, Riedel KD, Suda A, Ueda N, Janabi M, Mugusi F, Haefeli WE, Bertilsson L, Burhenne J, Aklillu E. 2011. Effect of rifampicin and CYP2B6 genotype on long-term efavirenz autoinduction and plasma exposure in HIV patients with or without tuberculosis. Clin Pharmacol Ther 90:406–413. https://doi.org/10.1038/clpt.2011.129.
38. Ngaimisi E, Mugusi S, Minzi OM, Sasi P, Riedel KD, Suda A, Ueda N, Janabi M, Mugusi F, Haefeli WE, Burhenne J, Aklillu E. 2010. Long-term efavirenz autoinduction and its effect on plasma exposure in HIV patients. Clin Pharmacol Ther 88:676–684. https://doi.org/10.1038/clpt.2010.172.
39. Han PY, Duffull SB, Kirkpatrick CM, Green B. 2007. Dosing in obesity: a simple solution to a big problem. Clin Pharmacol Ther 82:505–508. https://doi.org/10.1038/sj.clpt.6100381.
40. Dhoro M, Zvada S, Ngara B, Nhachi C, Kadzirange G, Chonzi P, Masimirembwa C. 2015. CYP2B6*6, CYP2B6*18, body weight and sex are predictors of efavirenz pharmacokinetics and treatment response: population pharmacokinetic modeling in an HIV/AIDS and TB cohort in Zimbabwe. BMC Pharmacol Toxicol 16:4. https://doi.org/10.1186/s40360-015-0004-2.
41. Desta Z, Saussele T, Ward B, Blievernicht J, Li L, Klein K, Flockhart DA, Zanger UM. 2007. Impact of CYP2B6 polymorphism on hepatic efavirenz metabolism in vitro. Pharmacogenomics 8:547–558. https://doi.org/10.2217/14622416.8.6.547.
42. Lang T, Klein K, Fischer J, Nussler AK, Neuhaus P, Hofmann U, Eichelbaum M, Schwab M, Zanger UM. 2001. Extensive genetic polymorphism in the human CYP2B6 gene with impact on expression and function in human liver. Pharmacogenetics 11:399–415. https://doi.org/10.1097/00008571-200107000-00004.
43. Lamba V, Lamba J, Yasuda K, Strom S, Davila J, Hancock ML, Fackenthal JD, Rogan PK, Ring B, Wrighton SA, Schuetz EG. 2003. Hepatic CYP2B6 expression: gender and ethnic differences and relationship to CYP2B6 genotype and CAR (constitutive androstane receptor) expression. J Pharmacol Exp Ther 307:906–922. https://doi.org/10.1124/jpet.103.054866.
44. Csajka C, Marzolini C, Fattinger K, Decosterd LA, Fellay J, Telenti A, Biollaz J, Buclin T. 2003. Population pharmacokinetics and effects of efavirenz in patients with human immunodeficiency virus infection. Clin Pharmacol Ther 73:20–30. https://doi.org/10.1067/mcp.2003.22.
45. Marzolini C, Sabin C, Raffi F, Siccardi M, Mussini C, Launay O, Burger D, Roca B, Fehr J, Bonora S, Mocroft A, Obel N, Dauchy FA, Zangerle R, Gogos C, Gianotti N, Ammassari A, Torti C, Ghosn J, Chene G, Grarup J, Battegay M, Efavirenz, Obesity Project Team on behalf of Collaboration of Observational HIV Epidemiological Research Europe (COHERE) in EuroCoord. 2015. Impact of body weight on virological and immunological responses to efavirenz-containing regimens in HIV-infected, treatment-naive adults. AIDS 29:193–200. https://doi.org/10.1097/QAD.0000000000000530.
46. de Roche M, Siccardi M, Stoeckle M, Livio F, Back D, Battegay M, Marzolini C. 2012. Efavirenz in an obese HIV-infected patient—a report and an in vitro-in vivo extrapolation model indicate risk of underdosing. Antivir Ther 17:1381–1384. https://doi.org/10.3851/IMP2107.
47. Cho DY, Ogburn ET, Jones D, Desta Z. 2011. Contribution of N-glucuronidation to efavirenz elimination in vivo in the basal and rifampin-induced metabolism of efavirenz. Antimicrob Agents Chemother 55:1504–1509. https://doi.org/10.1128/AAC.00883-10.
48. Honorio Tda S, Pinto EC, Rocha HV, Esteves VS, dos Santos TC, Castro HC, Rodrigues CR, de Sousa VP, Cabral LM. 2013. In vitro-in vivo correlation of efavirenz tablets using GastroPlus®. AAPS PharmSciTech 14:1244–1254. https://doi.org/10.1208/s12249-013-0016-4.
49. Gao J, Hussain MA, Motheram R, Gray DA, Benedek IH, Fiske WD, Doll WJ, Sandefer E, Page RC, Digenis GA. 2007. Investigation of human pharmacoscintigraphic behavior of two tablets and a capsule formulation of a high dose, poorly water soluble/highly permeable drug (efavirenz). J Pharm Sci 96:2970–2977. https://doi.org/10.1002/jps.20962.
50. Cristofoletti R, Nair A, Abrahamsson B, Groot DW, Kopp S, Langguth P, Polli JE, Shah VP, Dressman JB. 2013. Biowaiver monographs for immediate release solid oral dosage forms: efavirenz. J Pharm Sci 102:318–329. https://doi.org/10.1002/jps.23380.
51. Horter D, Dressman JB. 2001. Influence of physicochemical properties on

dissolution of drugs in the gastrointestinal tract. Adv Drug Deliv Rev 46:75–87. https://doi.org/10.1016/S0169-409X(00)00130-7.
52. Holford NH, Ambros RJ, Stoeckel K. 1992. Models for describing absorption rate and estimating extent of bioavailability: application to cefetamet pivoxil. J Pharmacokinet Biopharm 20:421–442. https://doi.org/10.1007/BF01061464.
53. Li J, Karlsson MO, Brahmer J, Spitz A, Zhao M, Hidalgo M, Baker SD. 2006. CYP3A phenotyping approach to predict systemic exposure to EGFR tyrosine kinase inhibitors. J Natl Cancer Inst 98:1714–1723. https://doi.org/10.1093/jnci/djj466.
54. Mukonzo JK, Okwera A, Nakasujja N, Luzze H, Sebuwufu D, Ogwal-Okeng J, Waako P, Gustafsson LL, Aklillu E. 2013. Influence of efavirenz pharmacokinetics and pharmacogenetics on neuropsychological disorders in Ugandan HIV-positive patients with or without tuberculosis: a prospective cohort study. BMC Infect Dis 13:261. https://doi.org/10.1186/1471-2334-13-261.
55. Sanchez Martin A, Cabrera Figueroa S, Cruz Guerrero R, Hurtado LP, Hurle AD, Carracedo Alvarez A. 2013. Impact of pharmacogenetics on CNS side effects related to efavirenz. Pharmacogenomics 14:1167–1178. https://doi.org/10.2217/pgs.13.111.
56. Gutierrez-Valencia A, Viciana P, Palacios R, Ruiz-Valderas R, Lozano F, Terron A, Rivero A, Lopez-Cortes LF, Sociedad Andaluza de Enfermedades Infecciosas. 2009. Stepped-dose versus full-dose efavirenz for HIV infection and neuropsychiatric adverse events: a randomized trial. Ann Intern Med 151:149–156. https://doi.org/10.7326/0003-4819-151-3-200908040-00127.
57. Wagner DR, Heyward VH. 2000. Measures of body composition in blacks and whites: a comparative review. Am J Clin Nutr 71:1392–1402.
58. Michaud V, Kreutz Y, Skaar T, Ogburn E, Thong N, Flockhart DA, Desta Z. 2014. Efavirenz-mediated induction of omeprazole metabolism is CYP2C19 genotype dependent. Pharmacogenomics J 14:151–159. https://doi.org/10.1038/tpj.2013.17.
59. Michaud V, Ogburn E, Thong N, Aregbe AO, Quigg TC, Flockhart DA, Desta Z. 2012. Induction of CYP2C19 and CYP3A activity following repeated administration of efavirenz in healthy volunteers. Clin Pharmacol Ther 91:475–482. https://doi.org/10.1038/clpt.2011.249.
60. Beal S, Sheiner LB, Boeckmann A, Bauer RJ. 2009. NONMEM user's guides (1989-2009). Icon Development Solutions, Ellicott City, MD.
61. Holford N. 2014. Wings for NONMEM v.7 for NONMEM 7.3. http://wfn.sourceforge.net/. Accessed 5 August 2016.
62. Lindbom L, Pihlgren P, Jonsson EN. 2005. PsN-Toolkit—a collection of computer intensive statistical methods for non-linear mixed effect modeling using NONMEM. Comput Methods Programs Biomed 79:241–257. https://doi.org/10.1016/j.cmpb.2005.04.005.
63. Keizer RJ, Karlsson MO, Hooker A. 2013. Modeling and simulation workbench for NONMEM: tutorial on Pirana, PsN, and Xpose. CPT Pharmacometrics Syst Pharmacol 2:e50. https://doi.org/10.1038/psp.2013.24.
64. R Development Core Team. 2008. R: a language and environment for statistical computing. R Foundation for Statistical Computing, Vienna, Austria. http://www.R-project.org. Accessed 5 August 2016.
65. Anderson BJ, Holford NH. 2009. Mechanistic basis of using body size and maturation to predict clearance in humans. Drug Metab Pharmacokinet 24:25–36. https://doi.org/10.2133/dmpk.24.25.
66. Anderson BJ, Holford NH. 2008. Mechanism-based concepts of size and maturity in pharmacokinetics. Annu Rev Pharmacol Toxicol 48:303–332. https://doi.org/10.1146/annurev.pharmtox.48.113006.094708.
67. West GB, Brown JH, Enquist BJ. 1997. A general model for the origin of allometric scaling laws in biology. Science 276:122–126. https://doi.org/10.1126/science.276.5309.122.